

$^{19}\text{F}(d, \alpha_0) ^{17}\text{O}$ and $^{19}\text{F}(d, \alpha_1) ^{17}\text{O}$ reaction excitation function measurements between 2.34 and 14.45 MeV†

R. E. Bigler,* S. A. A. Zaidi, J. L. Horton,‡ and H. Seitz
Center for Nuclear Studies, University of Texas at Austin, Texas 78712
(Received 17 April 1975)

The $^{19}\text{F}(d, \alpha_0) ^{17}\text{O}$ and $^{19}\text{F}(d, \alpha_1) ^{17}\text{O}$ reactions have been studied by measuring excitation functions in 30 keV steps over the energy range between 2.34 and 14.45 MeV deuteron energies. Cross-section data were collected simultaneously at laboratory angles of 70°, 90°, 120°, 150°, and 170°. The measured excitation functions exhibit strong resonance structures superimposed upon a smoothly varying component. The widths of these resonances are on the order of 500 keV. The corresponding excitation energy of the compound nucleus ^{21}Ne ranged between 19 and 25 MeV. A narrow region encompassing one of the strongest resonances was measured in smaller steps to look for finer structure. No evidence for fine structure greater than 10 keV was observed.

NUCLEAR REACTIONS $^{19}\text{F}(d, \alpha_{0,1})$, $E_d=2.34-14.45$ MeV, measured excitation functions at five laboratory angles. Deduced direct reaction contribution of reaction mechanism.

I. INTRODUCTION

A number of authors have investigated the $^{19}\text{F}(d, \alpha) ^{17}\text{O}$ reaction in order to understand the nature of the interaction mechanism. At energies up to 1.25 MeV the total cross sections were found¹ to be consistent with the $(2J+1)$ rule, as is expected from a statistical compound nucleus mechanism (SCN). Jahns, Nelson, and Bernstein² studied excitation functions and angular distributions in the 2.2 to 2.7 MeV energy range and found the total cross sections not to be proportional to $(2J+1)$, J being the spin of the final state. Similar measurements by El-Behay *et al.*³ from 1.1 to 2.3 MeV revealed evidence for ^{21}Ne compound nuclear resonances in the energy ranges 1.7 to 1.8 MeV and 2.1 to 2.2 MeV. Takeuchi *et al.*⁴ found good agreement to the $(2J+1)$ rule over the range 0.9 to 4.25 MeV for their total cross-section measurements. Their results confirmed the compound levels found at $E_d = 1.2$ to 1.8 MeV with width 600 keV and at $E_d = 2.3$ to 3.8 MeV with width 1.50 MeV. Recently, Zalyubovskii, Lobrovskii, and Vysotskii⁵ measured angular distributions and excitation functions over essentially the same energy range ($E_d = 1.0$ to 3.95 MeV). They observed three resonances at the respective energies $E_d = 1.7$, 2.2, and 2.7 MeV. A plane-wave Born approximation calculation including plane-wave pickup and plane-wave heavy particle stripping was used to show that the direct reaction mechanism is important in this energy region.

Angular distributions measured using a cyclotron at several energies between 5.5 and 20.9 MeV⁶⁻¹⁰ have been analyzed primarily in terms of a two-

nucleon pickup direct reaction mechanism.

Cosper, Lucas, and Johnson⁸ found that incoherent addition of an isotropic SCN component and a plane-wave direct reaction component gave a fit to the α_0 , α_2 , and α_4 angular distributions, but not to the α_1 or α_3 ones at 9.2 MeV. The direct reaction component included an incoherent sum of two-nucleon pickup and heavy-particle stripping mechanisms. Wesolowski *et al.*⁹ attempted distorted-wave Born approximation (DWBA) fits at several energies between 5.5 and 11.5 MeV and found agreement only at the highest energy. Priest and Vincent¹⁰ obtained good DWBA fits at 20.9 MeV.

In order to better understand the reaction mechanisms involved in the $^{19}\text{F}(d, \alpha)$ reaction, excitation functions were measured over the range $E_d = 2.34$ to 14.45 MeV in 30 keV steps at laboratory angles 70°, 90°, 120°, 150°, and 170°. Excitation functions for the $^{19}\text{F}(d, \alpha_0)$ and $^{19}\text{F}(d, \alpha_1)$ reactions have been measured and analyzed. Experimental measurements for these reactions are compared with direct reaction contribution as a function of excitation energy. The direct reaction contribution was calculated using a two-nucleon-transfer DWBA.

II. EXPERIMENTAL PROCEDURE

The University of Texas CN injected EN tandem Van de Graaff provided the source of deuterons. After passing through a 90° analyzing magnet, the beam was focused onto a target at the center of a 102 cm diameter scattering chamber. Beam energy spread was estimated to be of the order of 5 keV or less. Fluorine targets were prepared by vacuum evaporation of NaF and BaF₂ onto approxi-

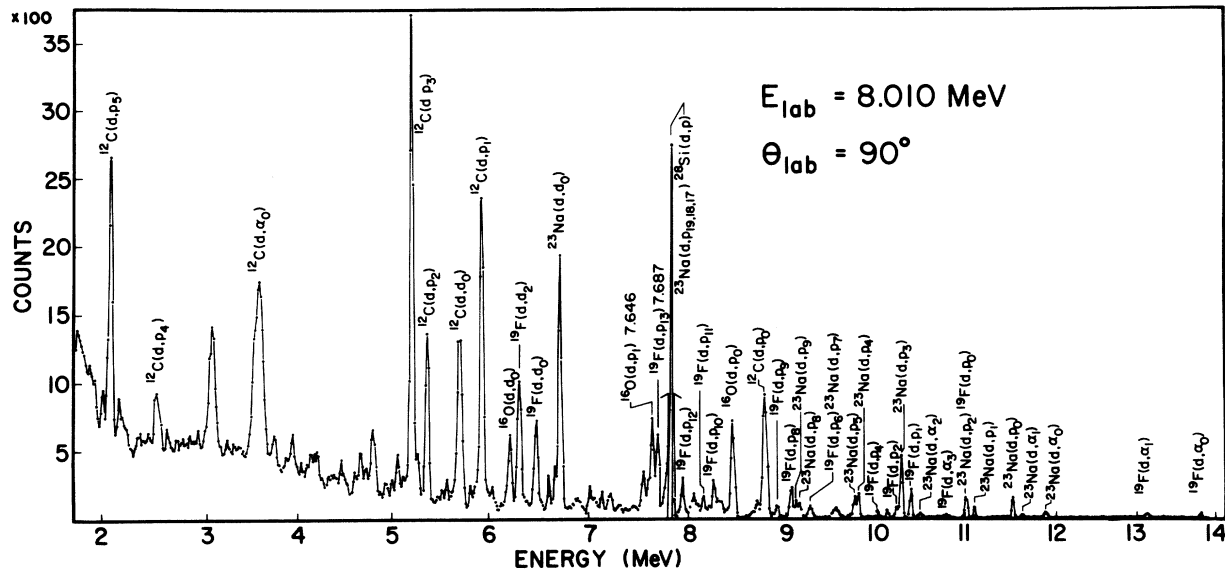


FIG. 1. Typical spectrum produced by deuteron scattering on an NaF target.

mately $5 \mu\text{g}/\text{cm}^2$ carbon foils. The fluorine content of the NaF target was approximately $15 \mu\text{g}/\text{cm}^2$. Five cooled lithium-drifted silicon detectors with an active area of 113 mm^2 and a depletion depth of 2.2 mm were used. Detector energy resolution was between 20 and 30 keV FWHM. The solid angles of the 70° , 90° , 120° , 150° , 170° detectors were, respectively, measured to be 0.58 , 0.58 , 0.71 , 0.71 , and 0.69 msr . The output of each detector, after suitable amplification, was routed to a PDP-7 computer for on-line storage. A typical spectrum obtained from an NaF target is shown in Fig. 1.

For the purpose of obtaining absolute cross sections, Rutherford scattering on the calcium component of a CaF_2 target was measured using 2.2 MeV deuterons at a laboratory scattering angle of 70° . The known relative calcium to fluorine content of this target determined the fluorine cross section. The ratio of fluorine deuteron elastic scattering in the CaF_2 target to that measured in the other targets at the same energy and angle was then used to obtain cross sections for the data taken from each different target. Our absolute cross sections are estimated to be accurate within 15% . Extensive checks of data reproducibility failed to reveal any evidence for target degradation in any of these targets.

A search for fine structure was attempted over a limited portion of the (d, α) excitation function. The target thickness in this energy range was approximately 5 keV . Data collection times were increased by a factor of 3 and the energy steps were reduced to 10 keV .

III. ANALYSIS AND RESULTS

A. Optical model

Optical potentials describing deuteron and α particle elastic scattering were required to generate the distorted waves for the DWBA analysis. Deuteron elastic scattering data on fluorine at 15.0 MeV were obtained from a paper by Dehnhard and Hintz.¹¹ Since elastic scattering α particle data on ^{17}O were unavailable, the $^{18}\text{O}(\alpha, \alpha_0)$ data of Lutz and Eccles¹² at 21.6 MeV were used.

Calculations were carried out using an optical model search program called FINDIT.¹³ The standard form of the optical potential was used, including a real Thomas-type spin-orbit part.

Dehnhard and Hintz¹¹ performed deuteron optical model fits without including a spin-orbit interaction term. The fits were good at forward angles, but poor beyond 110° . It was found that this poor back angle fit could be corrected by including a spin-orbit term in the optical potential. Sets A and C in Table I are FINDIT fits using their parameters. Set B shows that with further searching Set A can be slightly improved. Sets A and B correspond to including a surface imaginary absorption term while Set C corresponds to a volume absorption term. Using these parameters as a starting point, we began by performing a search including a spin-orbit term. Subsequently, all terms in the optical potential were allowed to vary independently until a stable χ^2 value was obtained. Sets D and E resulted from this procedure, respectively, for the surface and volume absorption cases. Both fits are shown in Fig. 2. To gain

TABLE I. Optical model parameters. $r_{so}=0.9$ fm and $a_{so}=0.6$ fm.

Reaction	Energy (MeV)	V (MeV)	W_w (MeV)	$4W_D$ (MeV)	V_{so} (MeV)	a_v (fm)	a_w (fm)	r_{0v} (fm)	r_{0w} (fm)	r_c (fm)	χ^2	Ref.
A $^{19}\text{F}(d, d)$	15.0	79.6	0.0	61.72	0.0	0.821	0.613	1.164	1.582	1.164	3.25	11
B $^{19}\text{F}(d, d)$	15.0	94.8	0.0	60.32	0.0	0.854	0.608	1.035	1.610	1.035	3.06	
C $^{19}\text{F}(d, d)$	15.0	94.3	7.49	0.0	0.0	0.806	0.560	1.027	2.175	1.027	3.31	11
D $^{19}\text{F}(d, d)$	15.0	94.4	0.0	46.8	4.94	0.858	0.626	1.006	1.615	1.006	1.64	
E $^{19}\text{F}(d, d)$	15.0	136.5	6.025	0.0	6.239	0.845	0.534	0.743	2.260	0.743	1.65	
F $\text{Ne}(d, d)$	11.6	136.8	7.47	0.0	4.32	0.780	0.700	0.732	2.065	0.732	1.44	
G $^{40}\text{Ca}(d, d)$	14.3	106.0	0.0	44.8	6.5	0.85	0.54	1.05	1.56	1.2		15
a $^{18}\text{O}(\alpha, \alpha)$	21.6	202.2	0.0	105.6	...	0.601	0.665	1.41	1.362	1.41	6.02	
b $^{18}\text{O}(\alpha, \alpha)$	21.6	204.4	27.4	0.0	...	0.604	0.662	1.40	1.338	1.40	5.97	
c $^{18}\text{O}(\alpha, \alpha)$	21.6	146.1	21.3	0.0	...	0.621	0.730	1.44	1.40	1.44	5.72	

further confidence in these fluorine parameters, the neon data of Jahr and Mairle¹⁴ were fitted, including a spin-orbit term. The resulting parameters were labeled set F. Comparison of Sets E and F parameters shows good agreement.

It is of interest to compare the surface fits of Set D with Set G. Set G parameters were obtained by Schwandt and Haerberli.¹⁵ Their parameters resulted from fits to data obtained from the elastic scattering of polarized and unpolarized deuterons on ^{40}Ca . It appears there is reasonable agreement in the relative size of the various parameters. This agreement gives further confidence that the addition of a spin-orbit term of this magnitude is

physically meaningful.

Since elastic scattering data on ^{17}O were not available, the 21.6 MeV $^{18}\text{O}(\alpha, \alpha)$ data of Lutz and Eccles¹² were used. Optical-model parameters for α particles can usually be found for various real well depths that give equally good data fits. In order to determine which parameters gave the best results in the DWBA calculations, optical-model fits at approximately $V=200$ MeV (Set a and Set B) for both surface and volume absorption, and at approximately $V=150$ MeV (Set C) for volume absorption, were calculated. It was found that in all cases the deeper well depths gave the best results.

Surface and volume fits for both the deuteron and

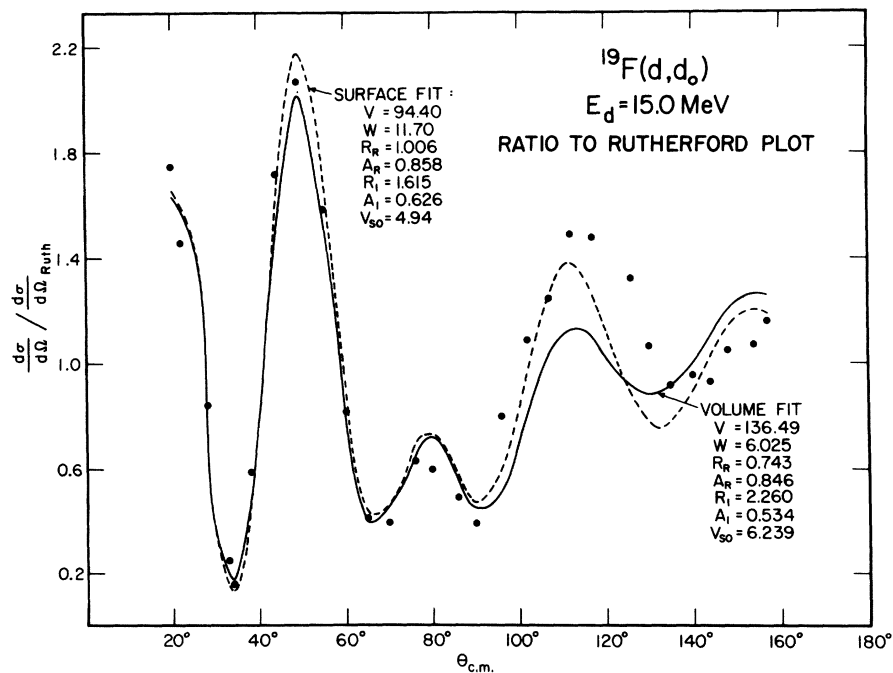


FIG. 2. Deuteron surface and volume optical model fits with spin-orbit interaction to the data of Dehnhard and Hintz (Ref. 11).

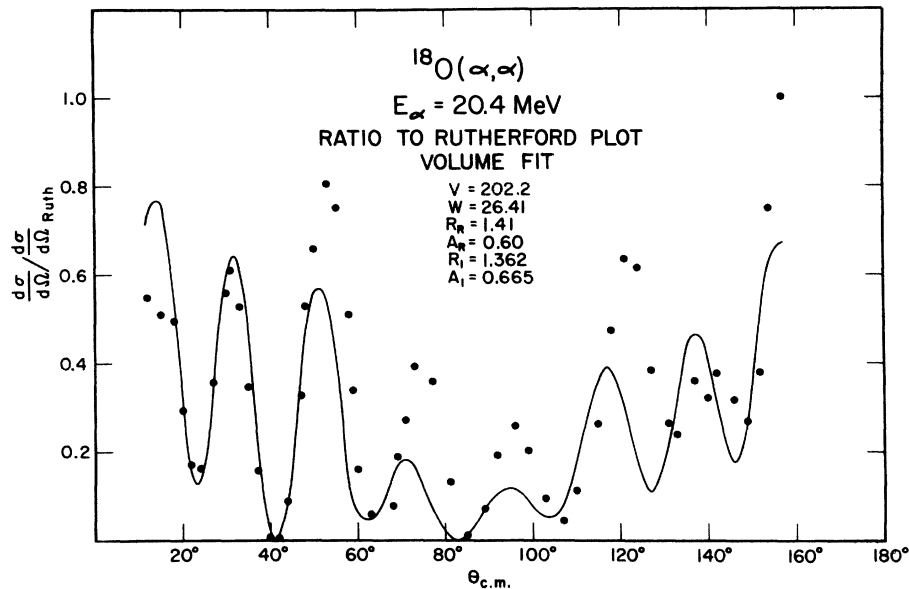


FIG. 3. α particle optical model fit to the data of Lutz and Eccles (Ref. 12).

α particle were obtained in order to determine which fit combination gave the best results in the DWBA calculations described below. The best over-all fits were obtained in all of the DWBA calculations when volume deuteron and volume α particle parameters were used. The variation was small, however, indicating that there is little sensitivity to the type of absorption. The result of the volume optical model α particle fit is shown in Fig. 3.

B. DWBA analysis

The purpose of the DWBA analysis was to estimate the direct reaction contribution to the $^{19}\text{F}(d, \alpha_0)^{17}\text{O}$ and $^{19}\text{F}(d, \alpha_1)^{17}\text{O}$ reaction cross sections over the entire energy region of our measurements. The direct reaction contribution through regions containing broad resonance structure was of special interest. Wesolowski *et al.*⁹ showed that a two-nucleon transfer analysis gave reasonable fits to their measured angular distributions only for the ground state transition at the highest energies of their measurements (11.5, 10.2, and 9.5 MeV). Priest and Vincent¹⁰ showed that a two-nucleon pickup reaction mechanism accounts for the differential cross section at 20.9 MeV. In order to obtain DWBA parameters including a spin-orbit interaction in the deuteron channel, we have refitted their angular distribution data using the computer code DWBA-VENUS.¹⁸ As pointed out by Priest and Vincent, this term should realistically be included but their computer code

did not have provision for its inclusion. The results of this calculation, which are of comparable quality to those obtained by Priest and Vincent, are shown in Fig. 4. Our DWBA calculations are normalized to the experimental cross sections of Priest and Vincent. This normalization and all DWBA parameters were held fixed while excitation functions were calculated over the entire range of and at the same laboratory angles as our measured excitation functions. The results of this calculation are displayed in Figs. 5–8 as dashed lines. Comparison between the calculations and the data above 10.0 MeV indicates the importance of direct two-nucleon pickup. It further follows that these calculations, extended into the energy region where resonances occur, may provide a reasonable estimate of the direct contribution there.

It has been found¹⁶ that a cluster model calculation is capable of determining the dominant orbital (l) and spin (j) angular momentum values for a (d, α) pickup reaction, when the magnitude of the contribution from different multipoles differs a good deal. The shape of the cluster form factor is then found to be nearly equal to a form factor calculated using a method that takes detailed nuclear structure information into account. Wesolowski *et al.*⁹ calculated form factors for the $^{19}\text{F}(d, \alpha_0)^{17}\text{O}$ and $^{19}\text{F}(d, \alpha_1)^{17}\text{O}$ reactions, taking microscopic nuclear structure of the target and residual nucleus into account. Their calculations showed the $l=2$ component to be about 85 times greater than the $l=4$ component for the ground state, and the

$l=0$ component about 9 times greater than the $l=2$ component for the first excited state. This information makes a simpler cluster calculation essentially equivalent to the more detailed treatment of Wesolowski *et al.*, and thus preferable for the present analysis.

The ^{19}F ground state is assumed to be a ^{16}O core plus three nucleons occupying $2s_{1/2}$, $1d_{3/2}$, and $1d_{5/2}$ levels with various amplitudes. These amplitudes have been calculated and listed by Wesolowski *et al.*⁹ The ^{17}O ground and first excited states are assumed to be an ^{16}O core plus a $1d_{5/2}$ neutron for the ground state and a $2s_{1/2}$ neutron

for the first excited state. Table II contains the final bound state parameters used in this analysis.

A cutoff radius has been employed by Priest and Vincent¹⁰ and Wesolowski *et al.*⁹ in their calculations; 4.58 fm and 5.27 fm, respectively. We found the quality of the angular distribution fits to worsen when either of these cutoffs were applied. Therefore, we did not use a cutoff radius in our calculations.

IV. DATA DISCUSSION

The $^{19}\text{F}(d, \alpha_0)^{17}\text{O}$ and $^{19}\text{F}(d, \alpha_1)^{17}\text{O}$ excitation function measurements are presented in Figs. 5–8. The higher energy regions for both reactions have been plotted with a factor of 2 increased scale. Above 10 MeV, evidence for resonance structure decreases. At lower energies there is considerable evidence for the presence of multiple overlapping resonance structure with widths of approximately 500 keV. This evidence becomes increasingly striking as the angle of observation is changed from forward to backward scattering angles.

Comparison of the measured and the calculated excitation functions in Figs. 5–8 shows that 10 MeV the calculated direct reaction cross sections account for a fair fraction of the observed cross sections. The discrepancies are more pronounced for the $^{19}\text{F}(d, \alpha_1)^{17}\text{O}$ reaction than for the $^{19}\text{F}(d, \alpha_0)^{17}\text{O}$ reaction. As the excitation energy is reduced this mechanism alone has greater and greater difficulty accounting for the entire cross section as can be seen in Figs. 5 and 7. At approximately 4 MeV, especially at the most backward laboratory angle, the broad resonance structures completely dominate the cross section.

A representative portion of the data collected in an attempt to reveal any fine structure riding on top of the broad resonance structure is shown in Fig. 9. The data labeled with dots correspond to a separate pass over the same energy region as the data labeled with x's. Clearly, no evidence for finer structure was found down to an upper limit of approximately 10 keV.

V. CONCLUSIONS

In light of previous $^{19}\text{F}(d, \alpha)$ data and the present extension, a number of conclusions may be

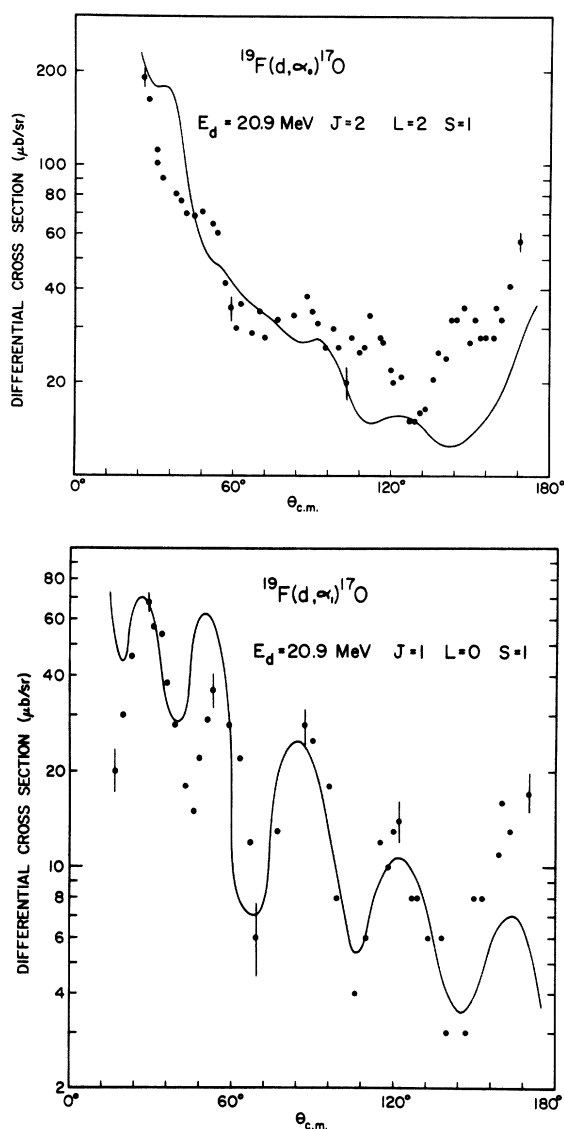
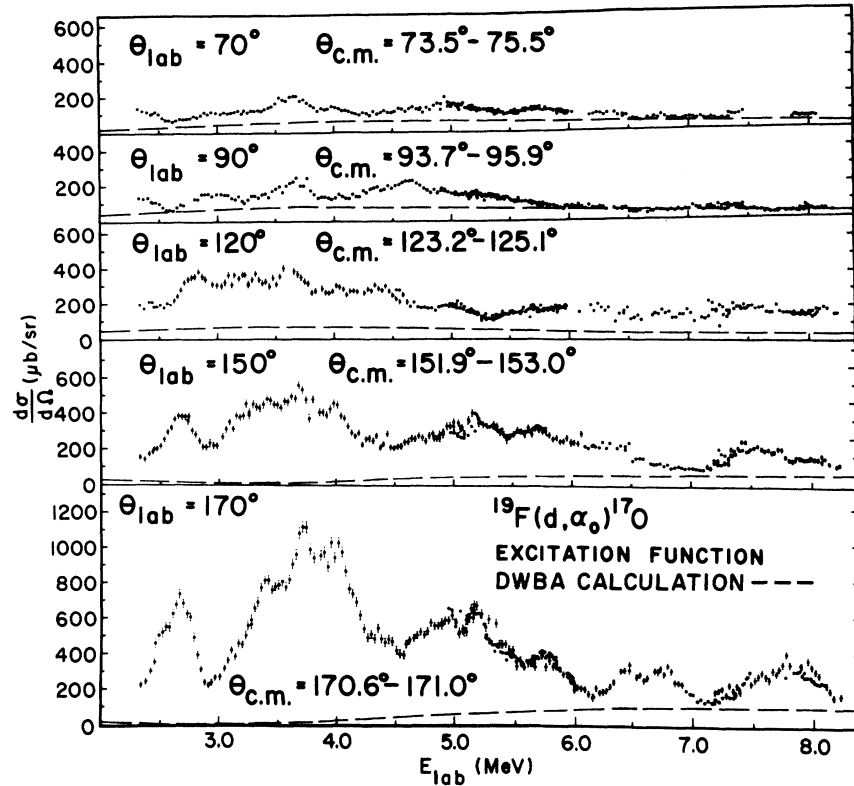
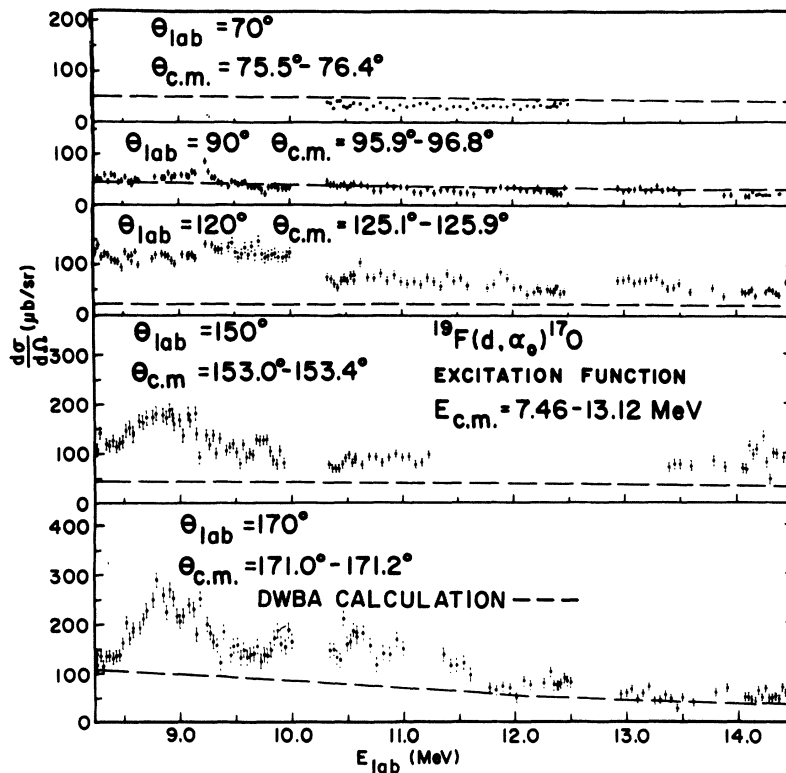


FIG. 4. DWBA fit to the 20.9 MeV $^{19}\text{F}(d, \alpha)^{17}\text{O}$ reaction data of Priest and Vincent (Ref. 10). Typical data error bars are included in the figure.

TABLE II. Bound state parameters.

Reaction	l	j	N	Binding				
				energy (MeV)	V_0 (MeV)	r_0 (fm)	a_0 (fm)	r_c (fm)
$^{19}\text{F}(d, \alpha_0)^{17}\text{O}$	2	2	3	13.814	138.1	1.3	0.9	1.33
$^{19}\text{F}(d, \alpha_1)^{17}\text{O}$	0	1	4	12.943	134.1	1.3	0.9	1.33

FIG. 5. Plot showing $^{19}\text{F}(d, \alpha_0)^{17}\text{O}$ excitation functions from 2.34 to 8.25 MeV.FIG. 6. Plot showing $^{19}\text{F}(d, \alpha_0)^{17}\text{O}$ excitation functions from 8.35 to 14.45 MeV.

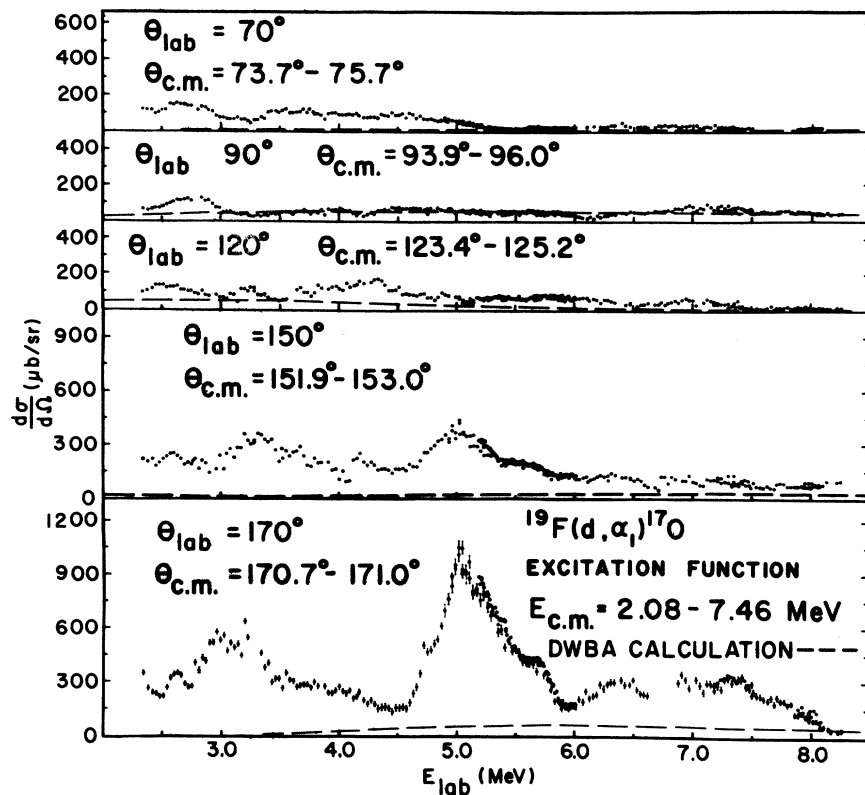


FIG. 7. Plot showing $^{19}\text{F}(d, \alpha)^{17}\text{O}$ excitation functions from 2.34 to 8.25 MeV.

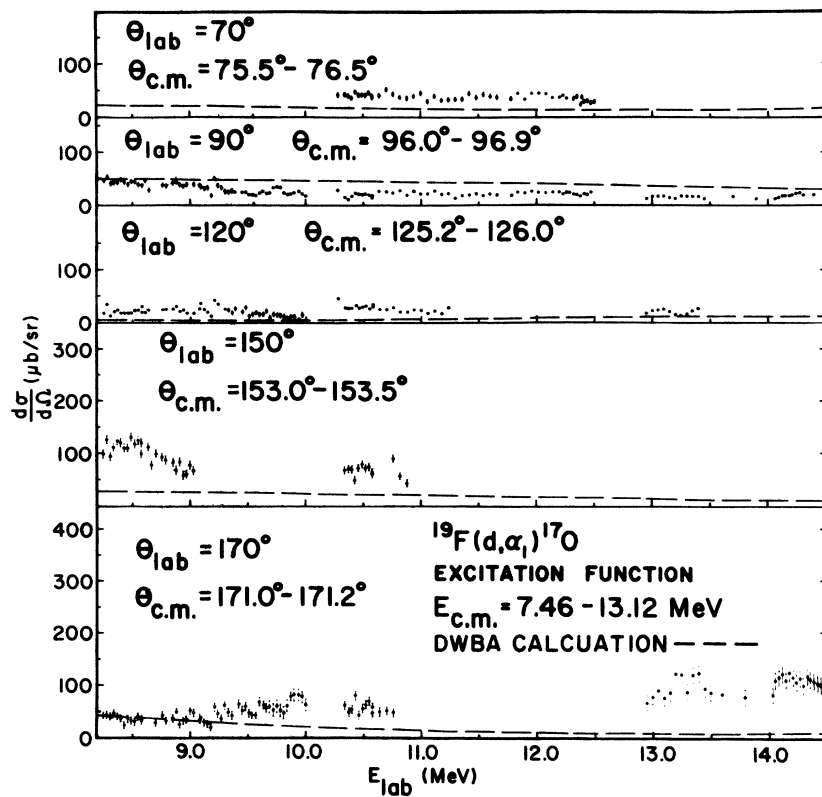


FIG. 8. Plot showing $^{19}\text{F}(d, \alpha)^{17}\text{O}$ excitation functions from 8.25 to 14.45 MeV.

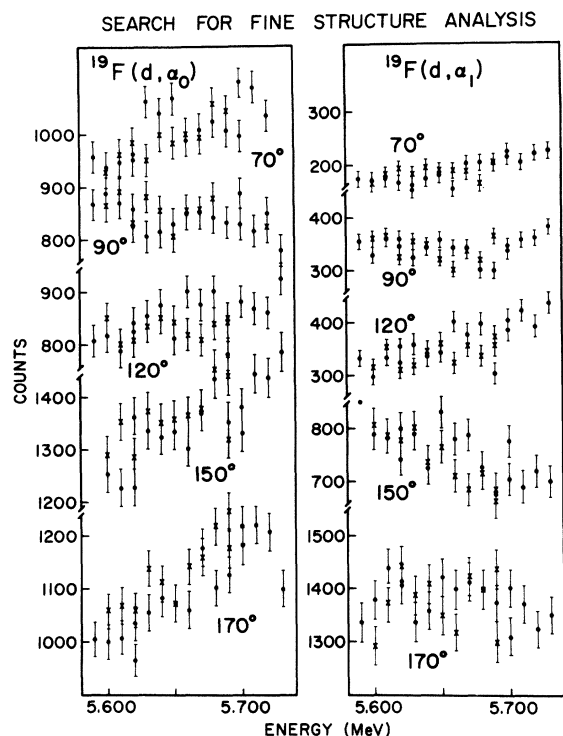


FIG. 9. Plot of $^{19}\text{F}(d, \alpha_0)^{17}\text{O}$ and $^{19}\text{F}(d, \alpha_1)^{17}\text{O}$ excitation functions which set an upper limit on the possibility of fine structure in these reactions. The data labeled with dots correspond to a separate pass over the same energy region as the data labeled with x's.

drawn with regard to the reaction mechanism. Above 10 MeV the two-nucleon pickup is an important mechanism. This follows from the DWBA fits to the cyclotron data as well as our calculated fit to the excitation function data above 10 MeV. Below approximately 4 MeV the earlier data showed that all three reaction mechanisms contribute to some extent, i.e. SCN, individual levels of the compound nucleus, and direct reaction. The inclusion of the SCN mechanism rests primarily upon the validity of the $(2J+1)$ rule. This paper attempts to identify the relative importance of the direct reaction mechanism over the entire energy range investigated.

Our attempt to reveal finer structure than the broad approximately 500 keV structure did not have a positive result. Had finer structure been observed it would have had the following significance. First, an analysis of the fine structure fluctuations would have allowed an estimate of the SCN contribution. Second, it would have given clear evidence that the observed resonance structure is intermediate structure.

ACKNOWLEDGMENTS

We are grateful to W. R. Coker for many useful discussions, for providing a number of essential programs, and for carefully reading the manuscript. The capable assistance of M. Koike and S. Ali in taking data is appreciated.

†Work supported in part by the U. S. Energy Research and Development Administration, Contract No. E(11-1)-3521.

*Present address: Biophysics Department, Sloan-Kettering Institute for Cancer Research, New York, New York 10021.

‡Present address: Radiation Laboratory, Ballistics Research Laboratories, U. S. Army Aberdeen Proving Ground, Maryland 21005.

¹D. M. Stanojević, S. D. Cirlov, and M. M. Ninković, *Nucl. Phys.* **73**, 657 (1965).

²M. F. Jahns, J. B. Nelson, and E. M. Bernstein, *Nucl. Phys.* **59**, 314 (1964).

³A. Z. El-Behay, M. A. Farouk, M. H. Nassef, and I. I. Zaloubovsky, *Nucl. Phys.* **61**, 282 (1964).

⁴Y. Takeuchi, Y. Hiratate, K. Miura, T. Tohei, and S. Morita, *Nucl. Phys.* **A109**, 105 (1968).

⁵I. I. Zalyubovskii, A. P. Lobkovskii, and G. L. Vysotskii, *Izv. Akad. Nauk SSSR Ser. Fiz.* **33**, 2056 (1969) [*Bull. Acad. Sci. USSR Phys. Ser.* **33**, 1873 (1969)].

⁶C. Hu, *J. Phys. Soc. Jpn.* **15**, 1741 (1960).

⁷K. Takamatsu, *J. Phys. Soc. Jpn.* **17**, 896 (1962).

⁸S. W. Cosper, B. T. Lucas, and O. E. Johnson, *Phys. Rev.* **138**, B51 (1965).

⁹J. J. Wesolowski, L. F. Hansen, J. G. Vidal, and M. L. Stelts, *Phys. Rev.* **148**, 1063 (1966).

¹⁰J. R. Priest and J. S. Vincent, *Phys. Rev.* **167**, 933 (1968).

¹¹D. Dehnhard and N. M. Hintz, *Phys. Rev. C* **1**, 460 (1970).

¹²H. F. Lutz and S. F. Eccles, *Nucl. Phys.* **81**, 423 (1963).

¹³W. R. Smith, University of Southern California Report No. 1, 36-119 (1967) (unpublished).

¹⁴R. Jahr and G. Mairle, *Nucl. Phys.* **70**, 383 (1965).

¹⁵P. Schwandt and W. Haeberli, *Nucl. Phys.* **A123**, 401 (1969).

¹⁶J. R. Curry, W. R. Coker, and P. J. Riley, *Phys. Rev.* **185**, 1416 (1969).

¹⁷T. Tamura, W. R. Coker, and F. Rybicki, *Comput. Phys. Commun.* **2**, 94 (1971).